UMSHA Press

AJMB
Avicenna Journal of Medical Biochemistry

Avicenna J Med Biochem, 2023; 11(2):129-137. doi:10.34172/ajmb.2446

http://ajmb.umsha.ac.ir

Original Article

Structure-Based Virtual Screening of Cinnamic Acid Analogs Against RIPK3: Implications for Anti-Inflammatory Drug Discovery

Elham Khoshbin[1], Seyed Mohamad Soroosh Rahmani-Abidar[1], Shadi Moradi[2], Amir Taherkhani[3*], Hamed Karkehabadi[1*]

[1]Department of Endodontics, School of Dentistry, Hamadan University of Medical Sciences, Hamadan, Iran
[2]Department of Medical Immunology, School of Medicine, Hamadan University of Medical Science, Hamadan, Iran
[3]Research Center for Molecular Medicine, Hamadan University of Medical Sciences, Hamadan, Iran

Article history:
Received: June 21, 2023
Revised: August 17, 2023
Accepted: August 23, 2023
ePublished: October 16, 2023

***Corresponding authors:**
Amir Taherkhani,
Email: amir.007.taherkhani@gmail.com
Hamed Karkehabadi,
Email: hamed_karkehabadi@yahoo.com

Abstract

Background: A common oral inflammatory disease known as apical periodontitis (AP) is caused by the intrusion of microorganisms into the dental pulp, resulting in an inflammatory response and bone degradation in periapical tissues. A growing body of evidence indicates that the receptor-interacting serine-threonine kinase 3 (RIPK3) is closely associated with AP.

Objectives: This study sought to address the requirement for effective RIPK3 inhibitors by examining the potential of cinnamic acid natural metabolites capable of inhibiting RIPK3.

Methods: The binding affinity of 20 cinnamic acids to the RIPK3 active site was evaluated by using AutoDock 4.0 software. The most favorable scores were assigned to the highest-ranking cinnamic acids based on their $\Delta G_{binding}$ values to the RIPK3 catalytic domain. A 100-nanosecond (ns) computer simulation was performed using molecular dynamics for the most efficacious inhibitor of RIPK3, and the findings were contrasted with those obtained for free RIPK3. The Discovery Studio Visualizer tool was employed to showcase the interactions between the RIPK3 active site and the highest-ranking metabolites.

Results: The binding affinity of cynarin, rosmarinic acid (RosA), and chlorogenic acid (CGA) to the RIPK3 active site was noteworthy, as the $\Delta G_{binding}$ values were<-10 kcal/mol. Furthermore, cynarin exhibited inhibition constant values at the picomolar range. Upon complexation with cynarin, the RIPK3 conformation attained stability after approximately 25 ns of simulation.

Conclusion: In general, cynarin, RosA, and CGA have the potential to be therapeutically beneficial in treating AP due to their ability to inhibit RIPK3.

Keywords: Apical periodontitis, Cinnamic acid, Drug, Inflammation, RIPK3

Please cite this article as follows: Khoshbin E, Rahmani-Abidar SMS, Moradi S, Taherkhani A, Karkehabadi H. Structure-based virtual screening of cinnamic acid analogs against RIPK3: implications for anti-inflammatory drug discovery. Avicenna J Med Biochem. 2023; 11(2):129-137. doi:10.34172/ajmb.2446

Background

Apical periodontitis (AP) is a prevalent oral inflammatory disease that is characterized by the microbial invasion of the dental pulp, leading to an inflammatory response and bone destruction in periapical tissues. This infectious ailment has a global prevalence and is a significant public health concern. Research has identified bacterial infection in the periapical area, particularly infections caused by *Fusobacterium nucleatum*, as a primary contributor to apical inflammation. *F. nucleatum* has been found to possess significant proinflammatory capabilities, further exacerbating the inflammatory response (1). It is noteworthy that approximately 50% of the adult population worldwide suffers from at least one tooth affected by AP. The manifestation of this dental condition is more conspicuous in samples collected from dental treatment facilities. However, it is also prevalent in samples obtained from the general population. These findings underscore the importance of increasing awareness and implementing preventative measures to address this prevalent oral health issue (2). Studies have demonstrated that microbial antigens derived from root canal infections can trigger both specific and non-specific immune responses in periapical tissues. Chronic periapical lesions arise from certain processes that impede host defense mechanisms from effectively eliminating the infection. Chronic periapical lesions serve as a mechanism to limit microbial invasion. However, despite the conduct

of experimental and clinical studies, factors, cells, and growth mediators that contribute to the development, maintenance, and resolution of these lesions remain incompletely understood (3). The root canal creates a favorable environment for anaerobic microorganisms to thrive and form a community with diverse biological and pathogenic properties, including antigenicity, mitogenic activity, chemotaxis, enzymatic histolysis, and the capacity to activate host cells. The presence of anaerobic microorganisms in the root canal can result in periapical inflammation when they spread or their products escape. In response, the host deploys a range of defenses, including various classes of cells, intercellular messengers, antibodies, and effector molecules. Despite the body's best efforts, it is often unable to eradicate the entrenched microbes in the root canal (4). Macrophages, being the first line of defense of the immune system against pathogen invasion, play a crucial role in regulating the inflammatory response. Recent studies have demonstrated that lipoteichoic acid (LTA) from *Enterococcus faecalis*, as well as heat-killed *E. faecalis* antigens, can stimulate the release of *tumor necrosis factor*-α (TNF-α) and nitric oxide (NO) in macrophages, potentially exacerbating the inflammatory response (5). Moreover, studies have revealed that LTA can activate the nucleotide-binding oligomerization domain-, leucine-rich repeat- and pyrin domain-containing protein 3 (NLRP3) inflammasome, and this activation is contingent on the nuclear factor Kappa B pathway (NF-κB) in macrophages (6). In response to bacterial infections, the immune system of the host organism induces cellular death. Necroptosis is a recently identified form of lytic cell death that exhibits significant proinflammatory and immunogenic properties (7). Microbial infection can manifest itself through a variety of symptoms, and two prominent forms of cell death, pyroptosis and necroptosis, are closely associated with this process (8). Necroptosis is a form of regulated cell death that has been discovered more recently than pyroptosis and does not depend on caspase activation. The necrosome complex, which is formed through the homotypic interaction motif of receptor-interacting protein and the activity of receptor-interacting serine-threonine kinase (RIPK) 1 and RIPK3, is necessary for the implementation of necroptosis. The necrosome complex, which is formed through the homotypic interaction motif of receptor-interacting protein and the activity of RIPK1 and RIPK3, is crucial for the execution of necroptosis. Cumulative evidence has demonstrated that the pathway involving the phosphorylation of RIPK3 is regulated tightly. This pathway then leads to the phosphorylation of mixed lineage kinase domain-like protein, which acts as the executor of necroptosis (7). The translocation of the RIPK3 phosphorylation pathway to the plasma membrane results in the permeabilization of the membrane, leading to the release of intracellular immunogenic contents and the stimulation of inflammatory responses (9).

Researchers have explored the use of naturally occurring substances as a potential source of therapeutic agents. Cinnamic acid, an essential aromatic carboxylic acid found in a variety of plants, including fruits, whole grains, vegetables, honey, *Cinnamomum cassia* (commonly known as Chinese cinnamon), and *Panax ginseng*, has been of particular interest (10). Studies suggest that cinnamic acids possess properties such as anti-inflammatory, anticancer, antibacterial, neuroprotective, and antioxidant effects. Cinnamic acid provides electrons that react with radicals to generate stable compounds, thereby disrupting chain reactions involving radicals (10).

In this study, cinnamic acid derivatives were chosen as the substrate for producing new derivatives due to their potential as the inhibitors of RIPK3, as well as the pharmacophoric requirements necessary for such inhibition. The binding affinity of permeability substances to the active site of RIPK3 was assessed by using the AutoDock 4.0 software.

Materials and Methods

Structural Preparation of the Receptor and Ligands

The relevant data were downloaded from the RCSB database (https://www.rcsb.org) (11,12) to retrieve the three-dimensional (3D) coordinates of RIPK3 (PDB ID: 7MON; X-ray resolution: 2.24 Å), which were then visualized using BIOVIA Discovery Studio Visualizer (DSV), version 19.1.0.18287. The PDB file contained two polypeptide chains (A and B). The first chain (A) consisted of 287 residues and was associated with the mixed lineage kinase domain-like protein, while the second chain (B) was selected for molecular docking simulations and corresponded to the structure of RIPK3, comprising 316 amino acids. The PDB file was processed using the Notepad + + software to remove water molecules and ZL1 (the positive control inhibitor; PubChem ID, 155524868). The DSV software was employed to analyze the docked pose of ZL1 in a 2D view, thereby enabling the identification of the active site interacting residues in 7MON. To achieve the most stable 3D conformation of the RIPK3 structure, 50 energy minimization runs were performed using Swiss-PdbViewer (version 4.1.0), accessible at https://spdbv.unil.ch. The protein's initial and final energy levels were determined to be -12980.640 and -15424.685 kJ/mol, respectively. A set of 20 natural cinnamic acids was chosen for determining potential RIPK3 inhibitors. The analysis of the RIPK3 active site entailed a comparison of the binding affinities of the studied cinnamic acids with that of ZL1. An energy minimization procedure was implemented on cinnamic acids in our earlier investigations (10,13,14).

Molecular Docking Analysis

A Windows-based PC with an Intel Core i5 processor, 16GB of installed RAM, and a 64-bit system type was used to conduct docking analyses (15). The $\Delta G_{binding}$ values (in kcal/mol units) between cinnamic acids, ZL1, and the RIPK3 binding site were computed by using the AutoDock tool (version 4.0) and a semi-flexible docking

algorithm (16). The RIPK3 active site contained several interacting residues such as Val27, Val35, Ala48, Lys50, Val52, Glu60, Met64, Leu92, Lys95, Phe96, Met97, Leu149, Ala159, Asp160, and Phe161. To facilitate the docking analysis, a grid box was established with some parameters (X-dimension, 68; Y-dimension, 64; Z-dimension, 50; X-center, -41.621 Å; Y-center, 4.48 Å; Z-center, -19.041 Å; and spacing, 0.375 Å). A total of 50 independent docked models were constructed for each ligand using the Lamarckian genetic algorithm to assess the binding affinity between the studied cinnamic acids, the positive control inhibitor, and the RIPK3 active site. The $\Delta G_{binding}$ *values* were clustered according to a root mean square (RMS) tolerance of 2.0 Å (17), and the most negative ΔGbinding value within the largest group was selected for evaluation. Subsequently, the DSV software was utilized to create molecular visualizations.

Molecular Dynamics Simulation

The preeminent RIPK3 inhibitor was selected for molecular dynamics (MD) simulation over a 100-nanosecond (ns) timespan, and the outcomes were juxtaposed against those obtained for free RIPK3. The enhanced configurations utilized in the computer simulations included several specifications; they were solvation model, explicit periodic boundary; cell shape, orthorhombic; minimum distance from the boundary, 10 angstroms; solvent, water; desired temperature, 310 Kelvin; force field, CHARMm; charge distribution, and point. The Discovery Studio Client (version 16.1.0.15350) was used for conducting the simulation. MD simulations were performed on a more powerful computer with certain specifications, including 64-bit system type, 64 GB DDR5 installed RAM, and an Intel 24-Core i9-13900KF processor. The root-mean-square deviation (RMSD) and the root-mean-square fluctuation (RMSF) of the RIPK3 backbone atoms were assessed to perform the MD analysis.

Interaction Mode Analysis

The top-ranked RIPK3 inhibitors were selected based on their $\Delta G_{binding}$ values. Compounds with a binding energy score of < -10 kcal/mol were identified as the most potent inhibitors of the enzyme and underwent interaction mode analysis using the DSV tool. The results were subsequently compared to those of the control inhibitor. Furthermore, the interactions between the highest-ranked RIPK3 inhibitor and the receptor residues were compared post-MD simulation.

Results

Binding Affinities Between Ligands and Receptor-Interacting Serine-threonine Kinase 3

The top-ranking RIPK3 inhibitors in this study were identified by determining the $\Delta G_{binding}$ value of the active site with three cinnamic acids, which was below -10 kcal/mol. The potential of cynarin, rosmarinic acid (RosA), and CGA as effective RIPK3 inhibitors was highlighted by their calculated binding energy values of -14.28, -11.63, and -10.90 kcal/mol, respectively. Based on the estimated *K*i values, cynarin was found to have a highly potent inhibitory effect on RIPK3, with a value within the picomolar (pM) range. Moreover, the inhibition exhibited by RosA and CGA was at the nanomolar (nM) level. The calculation of the $\Delta G_{binding}$ value between ZL1 and RIPK3 showed that cynarin had a higher binding affinity to the RIPK3 catalytic site compared to the reference inhibitor. The $\Delta G_{binding}$ value between ZL1 and RIPK3 was calculated as -13.18 kcal/mol (Figure 1). Table 1 provides the calculated $\Delta G_{binding}$ and *K*i values between RIPK3 and all ligands. The top-ranked cinnamic acids and the active site of RIPK3 were analyzed in detail, and all computed energy types are presented in Table 2. As stated in previous reports (18,19), the Gibbs free energy of binding between a small molecule and macromolecule is affected by different energies such as intermolecular energy, internal energy, torsional free energy, and the unbound system's energy.

MD Simulation

The RMSD of the RIPK3 backbone atoms was lower than that of unbound RIPK3, indicating that cynarin effectively stabilized the conformation of RIPK3. Additionally, Figure 2a illustrates that the structure of RIPK3 achieved stability after approximately 25 ns of computer simulation. As depicted in Figure 2b, RIPK3-cynarin demonstrated reduced fluctuation, particularly in the active site of the enzyme, compared to unbound RIPK3.

Interaction Modes

Interactions between the top-ranked cinnamic acids, ZL1, and residues located inside the RIPK3 active site underwent analysis. CGA formed the highest number of hydrogen bonds (n = 8) among the studied ligands, while RosA demonstrated the most hydrophobic interactions (n = 4) with the RIPK3 residues. ZL1 considerably formed

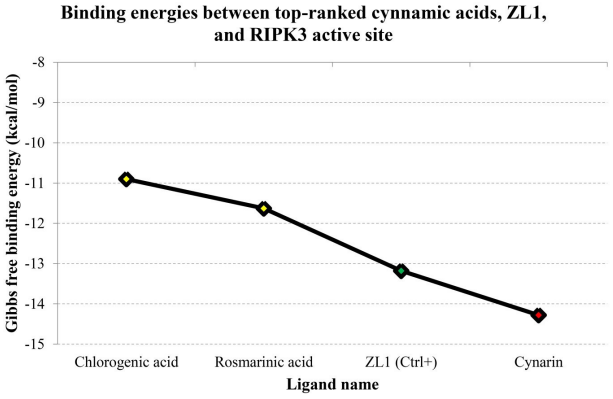

Figure 1. The Gibbs Free Binding Energy Between Top-ranked Cinnamic Acids, RIPK3 Positive Control Inhibitor, and the Active Site of the Receptor Indicated by the $\Delta G_{binding}$ Values in kcal/mol Units. *Note*. RIPK3: Receptor-interacting serine-threonine kinase 3. The X-axis of the graph displays the names of the ligands, while the corresponding Gibbs free binding energy is presented on the Y-axis. The green diamond symbolizes the positive control inhibitor, the red spot indicates the most potent RIPK3 inhibitors. In addition, the yellow spots illustrate compounds with a binding affinity to RIPK3, with $\Delta G_{binding}$ values of < -10 kcal/mol

6 hydrogen, 13 hydrophobic, 1 electrostatic, and 2 halogen interactions. The most potent RIPK3 inhibitor, cynarin, interacted with the RIPK3 active site through three hydrogen bonds and one hydrophobic interaction before MD simulation. Furthermore, cynarin established four hydrogen bonds and one hydrophobic interaction with the residues located within the RIPK3 active site. Among these interactions, the hydrogen bonds between Gly33, Ser101, and cynarin remained stable even after the MD simulation. The interactions between the ligands and the residues of the RIPK3 active site are summarized in Table 3 and shown in Figure 3. Figure 4 displays the overlaid configuration of the RIPK3 complex in association with cynarin before and after the MD simulation.

Table 1. The Gibbs Free Energy and *Ki* Values of the RIPK3 Active Site Assessed in the Presence of 20 Cinnamic Acids and a Positive Control Inhibitor

Ligand ID	Ligand Name	Binding Energy (kcal/mol)	*Ki*
6124212	Cynarin	-14.28	34.33 pM
5281792	Rosmarinic acid	-11.63	2.99 nM
1794427	Chlorogenic acid	-10.90	10.20 nM
113809112	Cinnamyl caffeate	-9.55	100.00 nM
5281759	Caffeic acid 3-glucoside	-9.20	180.03 nM
160355	Roscovitine	-9.15	196.79 nM
5372945	N-p-Coumaroyltyramine	-9.10	214.09 nM
5281787	Caffeic acid phenethyl ester	-8.87	316.42 nM
5919576	Benzyl caffeate	-8.61	491.10 nM
5281787	Phenethyl caffeate	-8.21	954.03 nM
637540	o-Coumaric acid	-8.00	1.37uM
5472440	Artepillin C	-7.22	5.12 uM
689043	Caffeic acid	-7.12	6.06 uM
689075	Methyl caffeate	-6.84	9.73 uM
637542	p-Coumaric acid	-6.09	34.47uM
637775	Sinapinic acid	-5.94	44.35 uM
445858	Ferulic acid	-5.89	48.39 uM
6440361	Drupanin	-5.75	60.53 uM
444539	Cinnamic acid	-5.69	67.57uM
819020	2-Methylcinnamic acid	-5.47	97.43 uM
155524868	ZL1 (Ctrl+)	-13.18	219.38 pM

Note. RIPK3: Receptor-interacting serine-threonine kinase 3; ZL1: N-[4-({2-[(cyclopropanecarbonyl) amino]pyridin-4-yl}oxy)-3-fluorophenyl]-1-(4-fluorophenyl)-2-oxo-1,2-dihydropyridine-3-carboxamide; Ctrl: Control; *Ki*: Inhibition constant.

Discussion

Given the challenges associated with traditional drug discovery methods, computer-aided drug design and virtual screening have become valuable approaches for identifying promising compounds. By using this combinatorial technique, we can select a more accurate biological target, reducing the expenses and duration of trials. In the current study, a target-specific computational method was used to identify effective RIPK3 ligands with innovative chemical structures (20).

Periodontal diseases that lead to adult tooth loss are caused by inflammatory processes initiated by complex bacterial colonies found in dental plaque. Many plant products have demonstrated noticeable anti-inflammatory properties, with *Schisandra chinensis* and its primary lignan Schisandrin C having anti-inflammatory effects that can suppress the expression of *interleukin* (IL)-1β and TNF-α and reduce NO production by human dental pulp cells in the presence of bacterial lipopolysaccharides (LPS). This botanical product has the potential to aid in treating oral-related inflammations such as pulpitis (21,22).

Earlier studies have documented the prospective inhibitory impact of cinnamic acids on MAPK3 (13) and MMP9 (10), implying their potential involvement in anti-inflammatory signaling pathways, aligning with our own discoveries. The findings of the present study revealed that cynarin, CGA, and RosA had a noteworthy binding affinity towards the RIPK3 active site. Cynarin, a biologically active functional group derivative of hydroxycinnamic acid found in certain plants and food, has been shown to possess pharmacological characteristics such as hypocholesterolemic, hepatoprotective, antiviral, antibacterial, and antihistamine effects (23). In the current investigation, cynarin displayed the most superior binding affinity compared to all the other mentioned cinnamic acid derivatives, with a binding energy value of -14.28 kcal/mol, and was associated with Gly33 (4.01), Ser101 (4.23), and Ser146 (3.77) amino acids via hydrogen bonds, while displaying hydrophobic interactions with Val27 (4.98). Kwon et al demonstrated that the extract derived from burdock, which contains cynarin, can reduce the levels of TNF-α, COX-2, and IL-6 expressions in periodontal diseases, effectively bringing them down to the levels exhibited by the control, indicating that the burdock extract has anti-inflammatory properties (21). Certain substances, including CGA, caffeic acid 3-glucoside, RosA, N-p-coumaroyltyramine, and caffeic

Table 2. Different Types of Energy Among the RIPK3 Active Site, Top-ranked Cinnamic Acids, and a Positive Control Inhibitor

Ligand Name	Final Intermolecular Energy (kcal/mol)	Final Total Internal Energy (kcal/mol)	Torsional Free Energy (kcal/mol)	Unbound System's Energy (kcal/mol)	Estimated Free Energy of Binding (kcal/mol)
Cynarin	-4.98	-17.58	6.26	-2.02	-14.28
Rosmarinic acid	-8.86	-8.26	4.47	-1.02	-11.63
Chlorogenic acid	-7.24	-9.37	4.18	-1.53	-10.90
ZL1 (Ctrl+)	-14.99	-0.68	1.79	-0.71	-13.18

Note. RIPK3: Receptor-interacting serine-threonine kinase 3; ZL1: N-[4-({2-[(cyclopropanecarbonyl) amino]pyridin-4-yl}oxy)-3-fluorophenyl]-1-(4-fluorophenyl)-2-oxo-1,2-dihydropyridine-3-carboxamide; Ctrl: Control.

Table 3. Interactions Between the Catalytic Site of RIPK3, Top-ranked Cinnamic Acids, and ZL1

Ligand Name	Hydrogen Bond (Distance in Angstrom)	Hydrophobic Interaction (Distance in Angstrom)	Electrostatic Interaction (Distance in Angstrom)	Halogen (Distance in Angstrom)
Cynarin (Before MD)	**Gly33 (4.01)**, **Ser101 (4.23)**, Ser146 (3.77)	Val27 (4.98)	Not found	Not found
Cynarin (After MD)	Asn147 (4.06), Ser101 (2.99), Gly33 (3.12, 4.14)	Lys50 (5.42)	Not found	Not found
Rosmarinic acid	Asp160 (3.79, 3.87, 4.11, 4.39), Met97 (4.08)	Lys50 (5.71), Leu73 (5.85), Ala48 (4.71), Ala 159 (6.60)	Not found	Not found
Chlorogenic acid	Asp160 (4.11, 4.23, 4.34, 4.53, 4.94), Asn147 (3.62, 4.22), Gly33(2.85)	Val35 (4.81), Ala159 (6.75), Leu149 (6.04)	Not found	Not found
ZL1 (Ctrl+)	Asp160 (4.04); Met97 (3.37, 4.33); Ala48 (3.61); Thr94 (4.17); Lys50 (4.41)	Val27 (5.80); Phe96 (5.76, 6.62); Met97 (6.08); Ala48 (4.19, 7.12); Leu149 (6.06); Val35 (6.98); Lys50 (3.95); Ala159 (5.96); Val52 (6.43); Leu92 (5.98); Phe161 (5.05)	Glu60 (4.97)	Ala48 (3.61); Thr94 (4.17)

Note. RIPK3: Receptor-interacting serine/threonine-protein kinase 3; MD: Molecular dynamics; ZL1: N-[4-({2-[(cyclopropanecarbonyl) amino]pyridin-4-yl}oxy)-3-fluorophenyl]-1-(4-fluorophenyl)-2-oxo-1,2-dihydropyridine-3-carboxamide; Ctrl: Control.

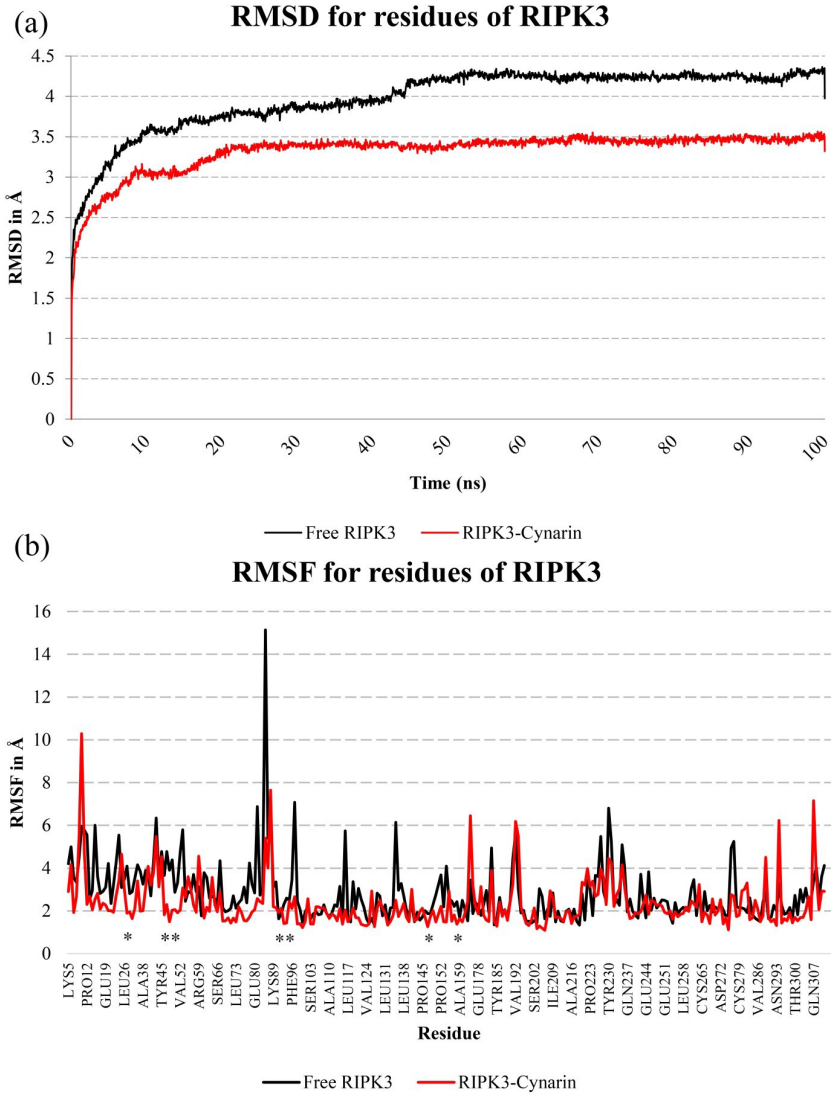

Figure 2. (a) RMSD and (b) RMSF of the Backbone Atoms of Free RIPK3 and RIPK3 in the Presence of Cynarin During the 100 ns MD Simulation. *Note*. RIPK3: Receptor-interacting serine-threonine kinase 3; RMSD: Root-mean-square deviation; RMSF: Root-mean-square fluctuation; MD: Molecular dynamics. The residues located within the RIPK3 active site are denoted with asterisks

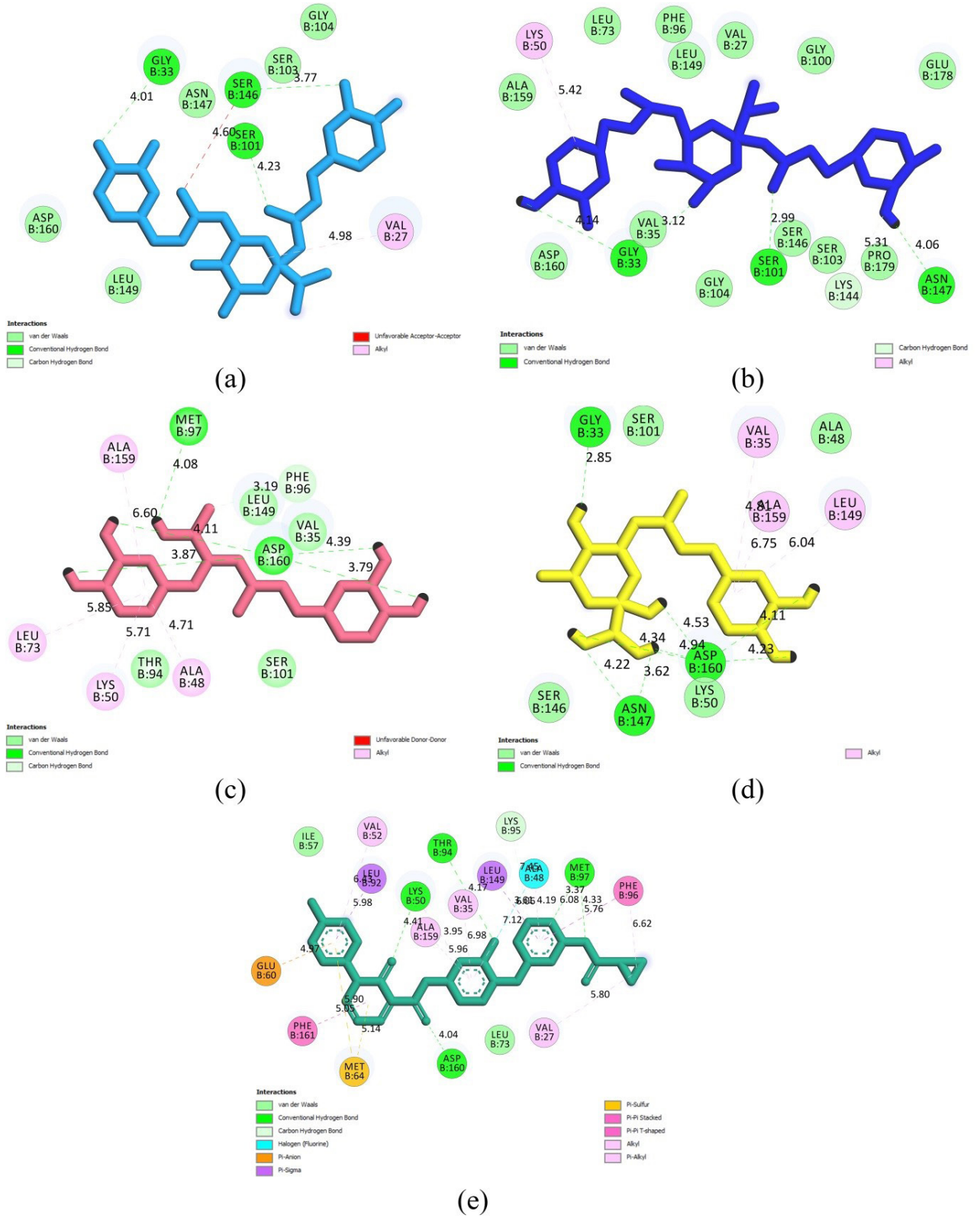

Figure 3. Interactions Between the Top-ranked Cinnamic Acids, ZL1, and Residues Inside the RIPK3 Active Site. *Note*. RIPK3: Receptor-interacting serine-threonine kinase 3; ZL1: N-[4-({2-[(cyclopropanecarbonyl) amino]pyridin-4-yl}oxy)-3-fluorophenyl]-1-(4-fluorophenyl)-2-oxo-1,2-dihydropyridine-3-carboxamide; MD: Molecular dynamics. Ligands are presented in (a) Cynarin before MD simulation, (b) Cynarin after MD simulation, (c) Rosmarinic acid, (d) Chlorogenic acid, and (e) ZL1

acid phenethyl ester, have been found to possess potential protective properties against tooth decay and peri-implant inflammation and diseases (14). Bousetla et al aimed to assess the phytochemical profiles of *Senecio angulatus* L.f. through in vitro tests to evaluate its antioxidant and anti-acetylcholinesterase activities. The extract was found to contain a significant amount of cynarin and trans-ferulic acid, with the butanolic extract having the highest concentration of CGA. Generally, phenolic compounds containing a hydroxyl group in their structure can

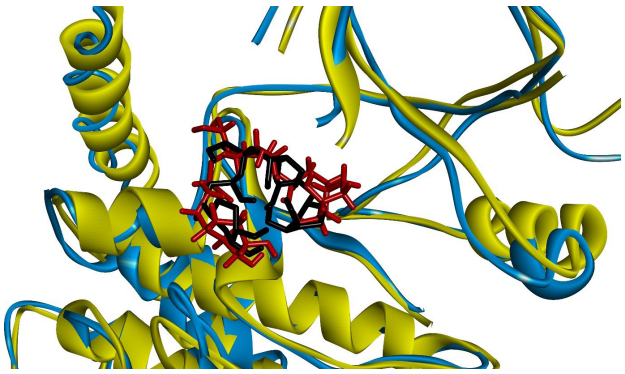

Figure 4. Superimposed Structures of RIPK3-cynarin Before and After MD Simulation. *Note*. RIPK3: Receptor-interacting serine-threonine kinase 3; MD: Molecular dynamics. Yellow and blue chains represent the protein before and after MD simulation, respectively. Black and red colors demonstrate the ligand before and after MD simulation, respectively

considerably contribute to antioxidant activities (24).

RosA, an ester derived from caffeic acid and 3,4-dihydroxyphenyllactic acid, indicates several noteworthy biological activities, including antiviral, antibacterial, anti-inflammatory, and antioxidant properties. It is commonly found in species of the Boraginaceae and the subfamily Nepetoideae of the Lamiaceae, as well as in various other higher plant families, fern, and hornwort species. The occurrence of RosA in medicinal plants, herbs, and spices has been correlated with various health-promoting and advantageous outcomes (25). In the present investigation, RosA exhibited the second-most elevated inclination, demonstrating a binding energy of -11.63 kcal/mol, forming a hydrogenic bond with Asp160 (3.79, 3.87, 4.11, 4.39) and Met97 (4.08) amino acids in RIPK3, while also representing a hydrophobic bond with a number of other amino acids (26). Ebselen and RosA, both topical anti-inflammatory drugs, were found to be successful in reducing gingival inflammation and plaque accumulation in a rhesus monkey model of plaque-induced gingivitis (26). The impacts of *Prunella vulgaris* L. (PVE) and its RosA composition on oxidative harm and inflammation in human gingival fibroblasts prompted by LPS have also been investigated by researchers. PVE and RosA were found to decrease the production of reactive oxygen species, the consumption of intracellular *glutathione*, and lipid peroxidation in treated cells with LPS, preventing the upregulation of IL-1β, IL-6, and TNF-α triggered by LPS, as well as inhibiting the expression of iNOS. These findings imply that PVE and RosA may decelerate the progression of periodontitis by mitigating the inflammatory response and the generation of oxidative mediators in gingival fibroblasts (27). A molecular docking analysis conducted to investigate targets and RosA, followed by establishing protein-protein interaction and drug-target-pathway networks using Cytoscape, revealed that RosA shows favorable biological activity and drug utilization, with 55 target genes being identified. These target genes are significantly associated with inflammatory response, tumor occurrence and development, and other biological processes. These findings highlight the potential of RosA to interact with a variety of proteins and pathways, establishing a comprehensive pharmacological network that can be effectively utilized for drug development. Finally, certain compounds, including RosA, cynarin, CGA, caffeic acid 3-glucoside, and N-p-coumaroyltyramine, have been suggested to potentially protect against dental caries and may be deemed as anti-caries agents (28-31).

CGA, an ester of cinnamic acids with quinic acid, is widely available and can be found in various foods such as tea and coffee. It exhibits strong antioxidant properties that can effectively ameliorate imbalanced intracellular redox state, leading to a decrease in the activation of the NF-κB signaling pathway and resulting in an anti-inflammatory reaction. It also has a variety of favorable attributes, including antibacterial, antiviral, anti-tumor, blood pressure-reducing, blood lipid-lowering, leukocyte-increasing, immune regulation-enhancing, as well as fragrance and color protection-enhancing functions. A study was conducted for the assessment of the binding energy of CGA, yielding a value of -10.9 kcal/mol, establishing it as the third most responsive among all cinnamic acid derivatives evaluated in the investigation. It was revealed to be connected with Asp160, Asn147, and Gly33 amino acids through hydrogen bonds, along with representing hydrophobic interactions with Val35, Ala159, and Leu149. The simultaneous administration of curcumin and CGA, a naturally occurring compound, has been shown to have a synergistic effect on reducing inflammation within a macrophage cell lineage through in vitro experimentation. Green tea polyphenols and honeysuckle CGA possess significant antibacterial and bactericidal properties, making them effective against common oral pathogens such as *S. mutans*, *P. gingivalis*, and *Staphylococcus* (32-35). Wang et al found that the crude extract of *Xanthium sibiricum* and its main active component CGA inhibited the activity of glucan transferase and the synthesis of water-soluble extracellular polysaccharide of *S. mutans*, indicating its potential as a natural anti-caries drug. Juwu et al discovered that CGA extracts from various plants demonstrated potent inhibitory properties against common bacterial strains and possessed antioxidant characteristics. In addition, Park et al concluded that CGA treatment had the effect of repressing the activation of TLR4/MyD88 and NF-κB in *Porphyromonas gingivalis* LPS-stimulated human gingival fibroblast cells. CGA also eliminated the LPS-induced phosphorylation of extracellular regulated kinase and protein kinase B (Akt), suggesting its potential to mitigate inflammatory responses by restraining TLR4/MyD88-mediated NF-κB, PI3K/Akt, and MAPK signaling pathways in these cells. Overall, CGA exhibits potential in inhibiting oral microorganisms, reducing inflammation, and possessing antioxidant properties, making it a promising candidate for natural anti-caries and anti-inflammatory drugs (33,36,37).

Conclusion

In light of the findings of this study, cynarin, RosA, and CGA represented potent inhibitory effects against RIPK3. Of these metabolites, cynarin stands out as the most potent, with *K*i values observed at the picomolar range. Upon binding with cynarin, the RIPK3 conformation achieved stability after undergoing approximately 25 ns of simulation. The findings of this study could be of significant relevance to researchers working towards the development of novel drug therapies for RIPK3-associated inflammatory disorders, including AP. It is important to acknowledge that the current findings require additional research to confirm their validity, which should include in vitro and in vivo validation experiments.

Acknowledgments

The authors thank the Research Center for Molecular Medicine, Hamadan University of Medical Sciences, Hamadan, Iran, for their support.

Authors' Contribution

Conceptualization: Amir Taherkhani.
Data curation: Amir Taherkhani, Seyed Mohamad Soroosh Rahmani-Abidar.
Formal analysis: Amir Taherkhani, Seyed Mohamad Soroosh Rahmani-Abidar.
Investigation: Amir Taherkhani, Elham Khoshbin, Hamed Karkehabadi.
Methodology: Amir Taherkhani, Seyed Mohamad Soroosh Rahmani-Abidar.
Project administration: Amir Taherkhani.
Resources: Amir Taherkhani.
Software: Amir Taherkhani, Seyed Mohamad Soroosh Rahmani-Abidar.
Supervision: Amir Taherkhani.
Validation: Amir Taherkhani, Elham Khoshbin, Hamed Karkehabadi.
Visualization: Amir Taherkhani, Elham Khoshbin, Hamed Karkehabadi.
Writing–original draft: Shadi Moradi.
Writing–review & editing: Amir Taherkhani, Elham Khoshbin, Hamed Karkehabadi.

Competing Interests

The authors declare that they have no competing interests.

Consent for Publication

Not applicable.

Data Availability Statement

The datasets used and/or analyzed during the current study are available from the corresponding author upon reasonable request.

Ethical Approval

The present study was approved by the Ethics Committee of Hamadan University of Medical Sciences, Hamadan, Iran (Ethics No. IR.UMSHA.REC.1402.216).

Funding

This research received no specific grant from any funding agency in the public, commercial, or not-for-profit sectors.

References

1. Amaral RR, Braga T, Siqueira JF Jr, Rôças IN, da Costa Rachid CTC, Oliveira AGG, et al. Root canal microbiome associated with asymptomatic apical periodontitis as determined by high-throughput sequencing. J Endod. 2022;48(4):487-95. doi: 10.1016/j.joen.2022.01.012.
2. Tibúrcio-Machado CS, Michelon C, Zanatta FB, Gomes MS, Marin JA, Bier CA. The global prevalence of apical periodontitis: a systematic review and meta-analysis. Int Endod J. 2021;54(5):712-35. doi: 10.1111/iej.13467.
3. Colić M, Gazivoda D, Vucević D, Vasilijić S, Rudolf R, Lukić A. Proinflammatory and immunoregulatory mechanisms in periapical lesions. Mol Immunol. 2009;47(1):101-13. doi: 10.1016/j.molimm.2009.01.011.
4. Nair PN. Pathogenesis of apical periodontitis and the causes of endodontic failures. Crit Rev Oral Biol Med. 2004;15(6):348-81. doi: 10.1177/154411130401500604.
5. Baik JE, Ryu YH, Han JY, Im J, Kum KY, Yun CH, et al. Lipoteichoic acid partially contributes to the inflammatory responses to *Enterococcus faecalis*. J Endod. 2008;34(8):975-82. doi: 10.1016/j.joen.2008.05.005.
6. Wang L, Jin H, Ye D, Wang J, Ao X, Dong M, et al. *Enterococcus faecalis* lipoteichoic acid-induced NLRP3 inflammasome via the activation of the nuclear factor kappa B pathway. J Endod. 2016;42(7):1093-100. doi: 10.1016/j.joen.2016.04.018.
7. Degterev A, Huang Z, Boyce M, Li Y, Jagtap P, Mizushima N, et al. Chemical inhibitor of nonapoptotic cell death with therapeutic potential for ischemic brain injury. Nat Chem Biol. 2005;1(2):112-9. doi: 10.1038/nchembio711.
8. Blériot C, Lecuit M. The interplay between regulated necrosis and bacterial infection. Cell Mol Life Sci. 2016;73(11-12):2369-78. doi: 10.1007/s00018-016-2206-1.
9. Dai X, Ma R, Jiang W, Deng Z, Chen L, Liang Y, et al. *Enterococcus faecalis*-induced macrophage necroptosis promotes refractory apical periodontitis. Microbiol Spectr. 2022;10(4):e0104522. doi: 10.1128/spectrum.01045-22.
10. Malekipour MH, Shirani F, Moradi S, Taherkhani A. Cinnamic acid derivatives as potential matrix metalloproteinase-9 inhibitors: molecular docking and dynamics simulations. Genomics Inform. 2023;21(1):e9. doi: 10.5808/gi.22077.
11. Burley SK, Bhikadiya C, Bi C, Bittrich S, Chen L, Crichlow GV, et al. RCSB Protein Data Bank: powerful new tools for exploring 3D structures of biological macromolecules for basic and applied research and education in fundamental biology, biomedicine, biotechnology, bioengineering and energy sciences. Nucleic Acids Res. 2021;49(D1):D437-D51. doi: 10.1093/nar/gkaa1038.
12. Chen CC, Herzberg O. Inhibition of beta-lactamase by clavulanate. Trapped intermediates in cryocrystallographic studies. J Mol Biol. 1992;224(4):1103-13. doi: 10.1016/0022-2836(92)90472-v.
13. Bayat Z, Tarokhian A, Taherkhani A. Cinnamic acids as promising bioactive compounds for cancer therapy by targeting MAPK3: a computational simulation study. J Complement Integr Med. 2023;20(3):621-30. doi: 10.1515/jcim-2023-0046.
14. Taherkhani A, Orangi A, Moradkhani S, Jalalvand A, Khamverdi Z. Identification of potential anti-tooth-decay compounds from organic cinnamic acid derivatives by inhibiting matrix metalloproteinase-8: an in silico study. Avicenna J Dent Res. 2022;14(1):25-32. doi: 10.34172/ajdr.2022.05.
15. Taherkhani A, Orangi A, Moradkhani S, Khamverdi Z. Molecular docking analysis of flavonoid compounds with matrix metalloproteinase-8 for the identification of potential effective inhibitors. Lett Drug Des Discov. 2021;18(1):16-45. doi: 10.2174/1570180817999200831094703.
16. Trott O, Olson AJ. AutoDock Vina: improving the speed and accuracy of docking with a new scoring function, efficient optimization, and multithreading. J Comput Chem. 2010;31(2):455-61. doi: 10.1002/jcc.21334.
17. Dinakarkumar Y, Rajabathar JR, Arokiyaraj S, Jeyaraj I, Anjaneyulu SR, Sandeep S, et al. Anti-methanogenic effect of

phytochemicals on methyl-coenzyme M reductase-potential: in silico and molecular docking studies for environmental protection. Micromachines (Basel). 2021;12(11):1425. doi: 10.3390/mi12111425.
18. Taherkhani A, Moradkhani S, Orangi A, Jalalvand A, Khamverdi Z. Molecular docking study of flavonoid compounds for possible matrix metalloproteinase-13 inhibition. J Basic Clin Physiol Pharmacol. 2020;32(6):1105-19. doi: 10.1515/jbcpp-2020-0036.
19. Khamverdi Z, Mohamadi Z, Taherkhani A. Molecular docking and dynamics simulation of natural phenolic compounds with GSK-3β: a putative target to combat mortality in patients with COVID-19. Recent Adv Inflamm Allergy Drug Discov. 2022;15(1):16-34. doi: 10.2174/1872213x14666210916161447.
20. Mahmud S, Parves MR, Riza YM, Sujon KM, Ray S, Tithi FA, et al. Exploring the potent inhibitors and binding modes of phospholipase A2 through in silico investigation. J Biomol Struct Dyn. 2020;38(14):4221-31. doi: 10.1080/07391102.2019.1680440.
21. Kwon K, Koong HS, Kang KH. Effect of burdock extracts upon inflammatory mediator production. Technol Health Care. 2016;24(3):459-69. doi: 10.3233/thc-151123 .
22. Takanche JS, Lee YH, Kim JS, Kim JE, Han SH, Lee SW, et al. Anti-inflammatory and antioxidant properties of Schisandrin C promote mitochondrial biogenesis in human dental pulp cells. Int Endod J. 2018;51(4):438-47. doi: 10.1111/iej.12861.
23. Raheem KS, Botting NP, Williamson G, Barron D. Total synthesis of 3,5-O-dicaffeoylquinic acid and its derivatives. Tetrahedron Lett. 2011;52(52):7175-7. doi: 10.1016/j.tetlet.2011.10.127.
24. Bousetla A, Keskinkaya HB, Bensouici C, Lefahal M, Atalar MN, Akkal S. LC-ESI/MS-phytochemical profiling with antioxidant and antiacetylcholinesterase activities of Algerian *Senecio angulatus* L.f. extracts. Nat Prod Res. 2023;37(1):123-9. doi: 10.1080/14786419.2021.1947274.
25. Petersen M, Simmonds MS. Rosmarinic acid. Phytochemistry. 2003;62(2):121-5. doi: 10.1016/s0031-9422(02)00513-7.
26. Van Dyke TE, Braswell L, Offenbacher S. Inhibition of gingivitis by topical application of ebselen and rosmarinic acid. Agents Actions. 1986;19(5-6):376-7. doi: 10.1007/bf01971261.
27. Zdarilová A, Svobodová A, Simánek V, Ulrichová J. Prunella vulgaris extract and rosmarinic acid suppress lipopolysaccharide-induced alteration in human gingival fibroblasts. Toxicol In Vitro. 2009;23(3):386-92. doi: 10.1016/j.tiv.2008.12.021.
28. Liu C, Mo L, Niu Y, Li X, Zhou X, Xu X. The role of reactive oxygen species and autophagy in periodontitis and their potential linkage. Front Physiol. 2017;8:439. doi: 10.3389/fphys.2017.00439.
29. Luo C, Zou L, Sun H, Peng J, Gao C, Bao L, et al. A review of the anti-inflammatory effects of rosmarinic acid on inflammatory diseases. Front Pharmacol. 2020;11:153. doi: 10.3389/fphar.2020.00153.
30. Guan M, Guo L, Ma H, Wu H, Fan X. Network pharmacology and molecular docking suggest the mechanism for biological activity of rosmarinic acid. Evid Based Complement Alternat Med. 2021;2021:5190808. doi: 10.1155/2021/5190808.
31. Taherkhani A, Ghonji F, Mazaheri A, Lohrasbi MP, Mohamadi Z, Khamverdi Z. Identification of potential glucosyltransferase inhibitors from cinnamic acid derivatives using molecular docking analysis: a bioinformatics study. Avicenna J Clin Microbiol Infect. 2021;8(4):145-55. doi: 10.34172/ajcmi.2021.27.
32. Naveed M, Hejazi V, Abbas M, Kamboh AA, Khan GJ, Shumzaid M, et al. Chlorogenic acid (CGA): a pharmacological review and call for further research. Biomed Pharmacother. 2018;97:67-74. doi: 10.1016/j.biopha.2017.10.064.
33. Wang Y, Zeng F, Liu X, Tian Y, Bai G. Effect of a new mouthwash based on Tea polyphenols and chlorogenic acid on dental caries and gingivitis. Pharmacol Res Mod Chin Med. 2022;3:100109. doi: 10.1016/j.prmcm.2022.100109.
34. Liang N, Kitts DD. Role of chlorogenic acids in controlling oxidative and inflammatory stress conditions. Nutrients. 2015;8(1):16. doi: 10.3390/nu8010016.
35. Bisht A, Dickens M, Rutherfurd-Markwick K, Thota R, Mutukumira AN, Singh H. Chlorogenic acid potentiates the anti-inflammatory activity of curcumin in LPS-stimulated THP-1 cells. Nutrients. 2020;12(9):2706. doi: 10.3390/nu12092706.
36. Juwu H, Xiaodan H, Xionghui L, Huang B. Antibacterial and antioxidant effects of three chlorogenic acid extracts. Med Plant. 2018;9(3).
37. Park CM, Yoon HS. Chlorogenic acid as a positive regulator in LPS-PG-induced inflammation via TLR4/MyD88-mediated NF-κB and PI3K/MAPK signaling cascades in human gingival fibroblasts. Mediators Inflamm. 2022;2022:2127642. doi: 10.1155/2022/2127642.